

PORTEVIN – LE CHATELIER EFFECT AND CAUSES OF REFRACTORINESS OF AUSTENITIC STEEL 08Kh18N8D3BR

A. A. Mogucheva,¹ I. A. Nikulin,¹ R. O. Kaibyshev,¹ and V. N. Skorobogatykh²

The mechanical behavior of steel 08Kh18N8D3BR in the temperature range of 500 – 740°C at deformation rates of 1.3×10^{-5} – 1.3×10^{-2} sec⁻¹ is studied. The conditions of manifestation of the Portevin – Le Chatelier effect in the steel are determined. The causes of the action of copper on the mechanical properties of the 18Cr – 8Ni-type steel are discussed.

Keywords: Portevin – Le Chatelier effect, austenitic steels, mechanical properties at elevated temperatures.

INTRODUCTION

Copper alloying of stainless steels of the austenitic class makes it possible to raise the temperature of their operation by 80 – 100°C [1, 2] and thus to use them as materials for the final heating loop and intermediate superheating loops of coal-fired power plants with operating steam temperature of 600 – 620°C (the operating temperature of the pipes is 650 – 680°C) [3]. Copper alloying provides a substantial gain in the long-term strength and creep resistance of austenitic steels of type 18 – 8 without lowering their good processibility and weldability. The Super304H steel developed by the Sumimoto Metals Ind. on the basis of steel 304L(N) with an additive of 3% Cu [2] is now the undoubted leader in the production of boilers of new-generation coal-fired power plants. Commercial success of the austenitic steel with 3% Cu has stimulated the development of a number of similar materials of which we should specially mention the Tempaloy AA1 steel created jointly by Kawasaki, Japan and TenarisNKK Tubes, Italy [4, 5]. It cannot be doubted that it is the introduction of copper that raises the characteristics of the high-temperature strength of austenitic steels [2 – 6]. However, the nature of the increase in the high-temperature properties of the austenitic chromium-nickel steels upon the introduction of copper remains unclear. Systematic data on the effect of copper on the creep resistance of austenitic steels are absent. Only in some works [2, 4 – 6] is it shown that coherent copper-bearing particles

with a size of about 10 nm are segregated in service of these steels for 3×10^3 – 2×10^4 h at elevated temperatures. The high creep resistance of austenitic steels with copper additives is connected with the reinforcing effect of these particles, the nature of which has not been determined. At the same time, it has been shown [5, 6] that any copper segregation is absent in the initial structure of the heat treated steel.

The present work is a part of a complex study aimed at determining the physical mechanisms ensuring high creep resistance in austenitic steels with 3% Cu.

The aim of the work consisted in studying the mechanical behavior of steel 08Kh18N8D3BR with composition close to that of Super304H in a wide range of temperatures and rates of deformation and determining the effect of copper on the nature of plastic strain in static tests of the steel.

METHODS OF STUDY

Stainless austenitic steel 08Kh18N8D3BR was die cast at the “TsNIIMASH” Company and had the following chemical composition (in wt.%): 0.09 C, 18.0 Cr, 8.13 Ni, 0.43 Nb, 0.17 N, 3.17 Cu, 0.98 Mn, 0.125 Si, 0.005 B.

The ingots were forged at 1180°C with a reduction ratio of 18.5. Hot-forged bars with cross section of 20 × 20 mm were subjected to standard commercial heat treatment [7], which included heating to 1150°C, 1-h hold at this temperature, and water cooling. This condition of the steel will be treated in the present paper as an initial one.

We performed mechanical tests of flat specimens with functional part with a length of 25 mm and cross section of 7 × 3 mm. The specimens were deformed in the equiaxed tension mode in an “INSTRON-5882” universal testing ma-

¹ Belgorod State University, Belgorod, Russia (E-mail: mogucheva@bsu.edu.ru).

² Central Research Institute for Machine Building Technology (GNTs RF OAO NPO “TsNIITMASH”), Moscow, Russia.

chine in the temperature range of 500 – 740°C at deformation rates of $1.3 \times 10^{-5} - 1.3 \times 10^{-2} \text{ sec}^{-1}$. The high-temperature tests were performed in a three-section furnace with separate control of zones. The temperature difference over the height of the furnace was $\pm 3^\circ\text{C}$. Before testing, the specimens were held in the furnace for 30 min at the test temperature. In order to increase the accuracy of the determination of mechanical properties we tested three specimens per one point. The scattering of the values of the conventional yield strength and of the rupture strength did not exceed 5 MPa. The elongation was measured using the hairlines deposited on the functional part of the specimens. The rate sensitivity factor was determined as $m = d \ln \sigma / d \ln \dot{\epsilon}$, where σ are the yielding stresses on the $\sigma - \epsilon$ curves obtained at different deformation rates $\dot{\epsilon}$ at the same strain. The strain hardening factor θ was determined in terms of the slope of the $\sigma - \epsilon$ curves by the formula [8]:

$$\theta = \frac{1}{4} \left(\frac{d\sigma}{d\epsilon} \right). \quad (1)$$

The relative error of measurement was 10%.

The structure of steel 08Kh18N8D3BR was studied in the initial condition and in the process of deformation at a rate of $1.3 \times 10^{-3} \text{ sec}^{-1}$ at 500 – 740°C. The microstructure was studied using an Olympus GX70 light microscope. The specimens for the metallographic studies were fabricated by the method of electrochemical polishing in a 30% solution of $\text{HNO}_3 + 70\% \text{ CH}_3\text{OH}$ at a voltage of 20 V. The electron microscope study was performed at an accelerating voltage of 200 kV in a JEM-2100 transmission electron microscope equipped with an attachment for energy dispersive analysis (Oxford Instruments). The secondary phases were identified using the diffraction patterns obtained from them and the results of chemical analysis. The foils for the electron microscope investigation were prepared by the method of jet chemical polishing in a solution of 10% $\text{HClO}_4 + 90\% \text{ CH}_3\text{COOH}$ in a TenuPol-5 device.

Differential scanning calorimetry (DSC) was applied to disc specimens with a weight of 34 mg using an SDT Q600 device (TA Instruments). The measurements were made in heating at a rate of 10 K/min.

The phase composition was simulated using the results of thermodynamic computations with the help of ThermoCalc software and the TCFE4 data base.

RESULTS

Initial Material. A typical structure of steel 08Kh18N8D3BR after standard heat treatment was represented by completely annealed austenite grains with a mean size of 18 μm (Fig. 1a). The dislocation density ρ was equal to $7 \times 10^{12} \text{ m}^{-2}$. The electron microscope study showed the presence of particles of second phases about 130 nm in size in the bodies of austenite grains; the particles have been

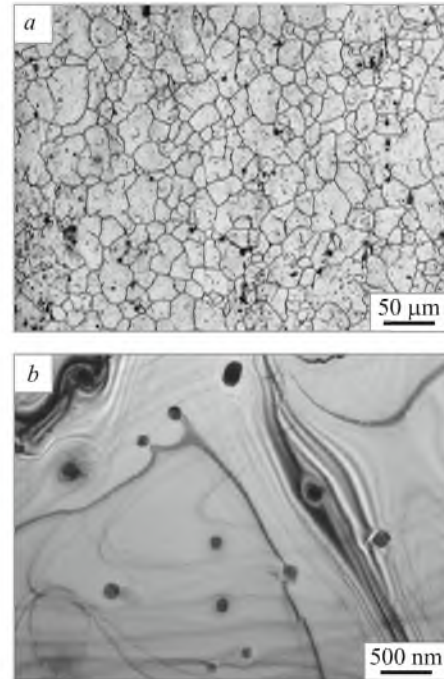


Fig. 1. Microstructure of steel 08Kh18N8D3BR after standard heat treatment: a) light metallography; b) transmission electron microscopy.

identified as primary segregations of Nb(C, N) carbonitrides. The presence of copper particles in the austenite matrix has not been detected by the method of electron microscopy. The data of DSC are presented in Fig. 2. The calorimetric curve obtained in heating exhibits a well manifested exothermic peak at 600°C. As a rule, this peak is associated with segregation of particles of secondary phases.

Mechanical Properties. The mechanical tests of steel 08Kh18N8D3BR performed at a deformation rate of $1.3 \times 10^{-3} \text{ sec}^{-1}$ showed that the straining of the specimens at 530 – 650°C was accompanied by discontinuous yielding

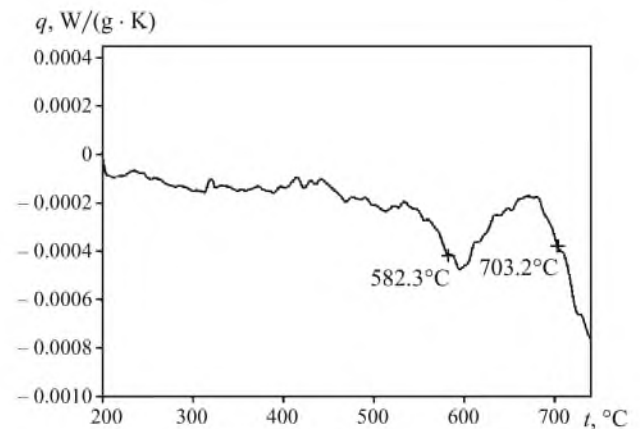


Fig. 2. DSC curve for steel 08Kh18N8D3BR obtained in heating to 750°C at a rate of 750 K/min (q is the derivative of the heat flux).

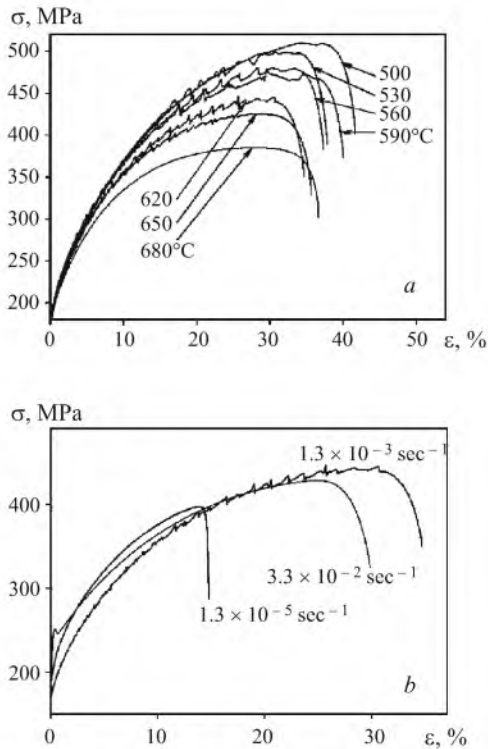


Fig. 3. Dependences of yielding stresses in steel 08Kh18N8D3BR on the strain due to deformation at a rate of $1.3 \times 10^{-3} \text{ sec}^{-1}$ in a temperature range of 500–680°C (*a*) and at a rate range of $1.3 \times 10^{-5} - 1.3 \times 10^{-2} \text{ sec}^{-1}$ at 620°C (*b*).

(DY), which manifested itself in a serrated form of the $\sigma - \epsilon$ curves (Fig. 3*a*). It is known that DY is a feature of the Portevin – Le Chatelier (PLC) effect [9]. At 530°C we observed type *E* discontinuous yielding [9], when the stress jumps occur with low strain hardening. In the range of 560 – 650°C DY develops by type *A* [9], which manifests itself in an abrupt growth in the yielding stresses and their abrupt decline.

Estimation of the effect of the rate of deformation on the form of the $\sigma - \epsilon$ curves in the metal deformed at 620°C in the range of $1.3 \times 10^{-5} - 1.3 \times 10^{-2} \text{ sec}^{-1}$ shows that the maximum rupture strength and ductility are exhibited by the steel deformed at $\dot{\epsilon} = 1.3 \times 10^{-3} \text{ sec}^{-1}$ and manifesting DY (Fig. 3*b*). Growth or decrease in the rate of deformation result in disappearance of DY and lowering of the strength and ductility. Note that in the whole studied range of deformation temperatures and rates, where steel 08Kh18N8D3BR exhibits DY, we observed only types *A* and *E* of discontinuous yielding. These types of DY are typical for the low-temperature and high-rate domain of existence of the PLC effect [9] and are connected with discontinuous formation of strain bands in one part of the deformed specimen and their propagation over the functional part of the specimen over one crystallographic direction. As a rule, steels of the austenitic class manifest other types of yielding in addition to the discontinuous yielding of types *A* and *E*. For example, yielding

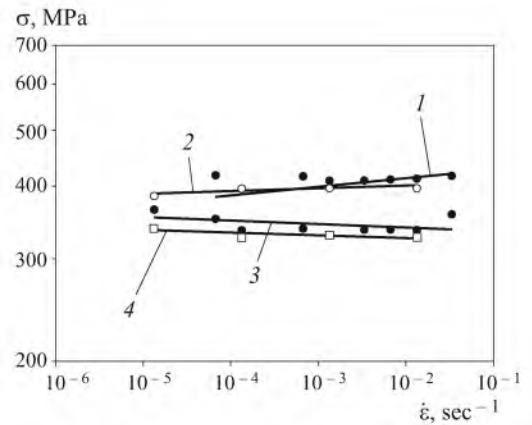


Fig. 4. Dependences of yielding stresses in steel 08Kh18N8D3BR on the rate of deformation: 1) factor of the rate sensitivity of yielding stress $m = 0.01$ at temperature $t = 620^\circ\text{C}$ and strain $\epsilon = 20\%$; 2) $m = 0.005$ at $t = 650^\circ\text{C}$ and $\epsilon = 20\%$; 3) $m = -0.06$ at $t = 620^\circ\text{C}$ and $\epsilon = 10\%$; 4) $m = -0.04$ at $t = 650^\circ\text{C}$ and $\epsilon = 10\%$.

of types *B* and *C* has been observed in the high-temperature and low-rate domain of existence of the PLC effect; these types are connected with dislocation glide within strain bands [9]. Discontinuous yielding of types *B* and *C* has not been detected for steel 08Kh18N8D3BR.

Thus, straining of steel 08Kh18N8D3BR is controlled by a specific mechanism weakly affected by the temperature and rate of deformation.

Figure 4 presents the dependences of the yielding stresses on the rate of deformation. The dependences are characterized by negative values of the factor of rate sensitivity m at low degrees of strain. This form of dependence of yielding stresses on the rate of deformation and negative values of factor m are typical for materials exhibiting the PLC effect [9].

It is known that the PLC effect is also characterized by a critical degree of strain ϵ_{cr} at which DY starts [10, 11]. Figure 5 presents the dependence of ϵ_{cr} on the temperature and rate of deformation. As the temperature grows, the values of ϵ_{cr} continuously tend to zero (Fig. 5*a*), exhibiting a “normal” behavior. The dependence of ϵ_{cr} on the rate of deformation $\dot{\epsilon}$ upon growth in $\dot{\epsilon}$ to $6.7 \times 10^{-4} \text{ sec}^{-1}$ is “normal.” At $\dot{\epsilon} > 6.7 \times 10^{-4} \text{ sec}^{-1}$ the dependence is “inverse.” In some works [10, 11] such dependence of ϵ_{cr} is associated either with cyclic segregation and dissolution of particles of a second phase or with formation and deterioration of short-range ordering.

The temperature dependences of the conventional yield strength $\sigma_{0.2}$, of the rupture strength σ_r , and of the elongation δ are presented in Table 1. It can be seen that in the temperature range of 500 – 740°C $\sigma_{0.2}$ remains invariable, δ varies within 3 – 4%, and σ_r exhibits a well manifested tendency to decrease upon growth in the temperature. At a temperature above 650°C the disappearance of DY, which results

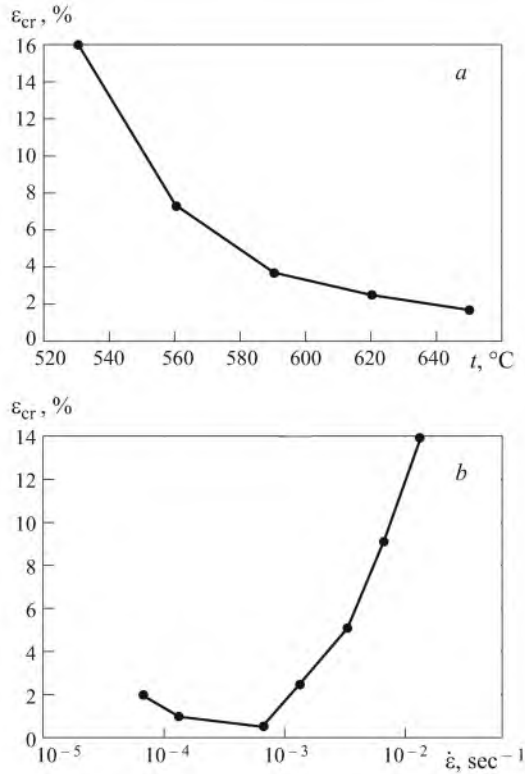


Fig. 5. Critical degree of strain ε_{cr} in steel 08Kh18N8D3BR as a function of the temperature (*a*) and rate (*b*) of deformation.

in a decrease in the strain hardening factor (Table 1), causes considerable lowering of σ_r .

In order to estimate the effect of copper alloying on the high-temperature strength, we compared the properties of three steels, namely, 08Kh18N8D3BR (the object of study), 304L (completely annealed [12, 13]), and TP347HFG (fine-grained [14]). The temperature dependence of the strength characteristics of the steels is presented in Fig. 6. It

TABLE 1. Mechanical Properties and Strain Hardening Factors of Steel 08Kh18N8D3BR Deformed at a Rate of $1.3 \times 10^{-3} \text{ sec}^{-1}$ at Various Temperatures

$t, ^\circ\text{C}$	$\sigma_{0.2}, \text{MPa}$	σ_r, MPa	$\delta, \%$	$\theta_{5\%}, \text{MPa}$	$\theta_{20\%}, \text{MPa}$
500	188	509	43	4.2	1.6
530	190	501	36	4.2	1.7
560	186	481	36	4.2	1.3
590	191	479	37	4.2	1.1
620	184	446	33	3.9	1.3
650	189	425	34	3.7	0.8
680	185	385	37	3.5	0.5
710	186	364	37	3.1	0.4
740	183	330	35	2.7	0.2

Notations: $\theta_{5\%}$ and $\theta_{20\%}$ are the strain hardening factors obtained at a strain of 5 and 20%, respectively.

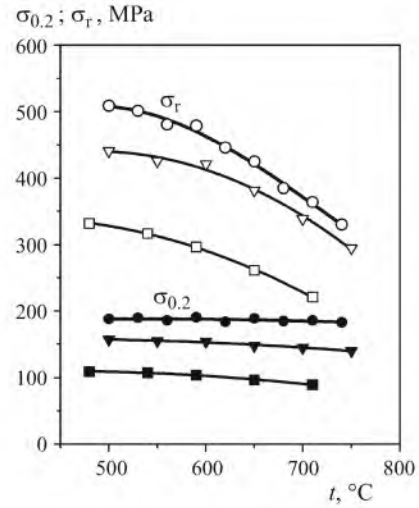


Fig. 6. Temperature dependences of mechanical properties of the following steels: \circ, \bullet) 08Kh18N8D3BR; \square, \blacksquare) 304L [11]; $\nabla, \blacktriangledown$) TP347HFG [13].

can be seen that the strength of the studied steel is higher than those of 304L and TP347HFG. The last steel contains 0.4% Nb, which is about equal to the content of niobium in 08Kh18N8D3BR. Upon growth in the test temperature the values of $\sigma_{0.2}$ for the studied steel remain constant, whereas in the other two steels they decrease (Fig. 6). In the temperature range of 500–740°C the value of $\sigma_{0.2}$ of steel 08Kh18N8D3BR is higher than in 304L and TP347HFG by about 90–100 and 30–40 MPa, respectively. Steel 08Kh18N8D3BR has high values of σ_r , which are about 1.6 and 1.1–1.2 times higher than in 304L and TP347HFG, respectively, in the whole temperature range studied (Fig. 6).

Microstructure after Deformation. Figure 7*a* presents a typical dislocation structure of steel 08Kh18N8D3BR deformed in the temperature and rate mode of existence of the PLC effect. It can be seen that extension to relatively low strain (about 30%) yields a well manifested low-energy dislocation structure in the form of strain bands. These bands differ from conventional strain-induced microbands [15] by a longer length. In addition to the observed serrated pattern of types *A* and *E*, this confirms that steel 08Kh18N8D3BR undergoes straining due to propagation of strain bands (plane slip). It should also be noted that the density of lattice dislocations accumulated in the metal during the deformation increases within one order of magnitude upon growth in the degree of strain from 5 to 30% (Table 2). At the same time, the dislocation density decreases with growth in the deformation temperature, which is connected with redistribution of lattice dislocations and formation of a low-energy dislocation structure (Fig. 7*a*). The data obtained correlate with the variation of σ_r in steel 08Kh18N8D3BR, the values of which have decreased upon growth in the temperature (Table 1 and Fig. 6).

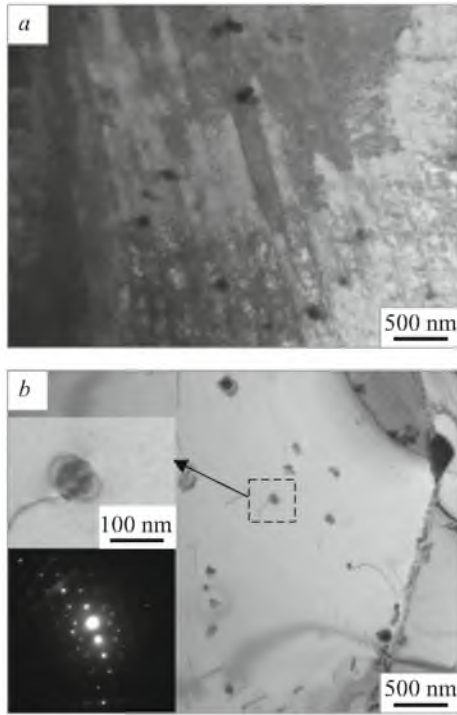


Fig. 7. Microstructure of steel 08Kh18N18D3BR deformed at a rate of $1.3 \times 10^{-3} \text{ sec}^{-1}$ at 620°C: *a*) functional part; *b*) region of grips.

The electron microscope study has not allowed us to give an unambiguous answer to the question of the nature of the exothermal peak in Fig. 2. It can be caused by segregation either of coherent particles of Nb(C, N) about 78 nm in size (Fig. 7*b*) or of copper nanoparticles. We can only be positive that the absolute majority of the particles segregating in the range of 530 – 680°C have coherent boundaries, the presence of which follows from the specific contrast from the elastic stresses on the austenitic matrix near the phase boundaries.

DISCUSSION

The results obtained show that alloying of the steel with niobium and copper produces a favorable effect on its strength. The introduction of niobium in an amount of 0.43% leads to formation of nanosize coherent particles that ensure precipitation hardening; the size of the copper particles is much smaller. It seems that the main contribution to the hardening is made by copper, which ensures high strength of steel 08Kh18N8D3BR at elevated temperatures.

Formation of coherent particles in the austenite matrix results in exceptionally high growth in the dislocation density in the initial stages of plastic yielding; at $\varepsilon \leq 5\%$ the dislocation density increases by about a factor of 50 as compared with the initial density (Table 2). In matrix alloys the growth in the dislocation density by a factor of 2 – 4 due to similar degrees of strain is assumed to be high [16]. This feature of steel 08Kh18N8D3BR is explainable only by the fact

TABLE 2. Dislocation Density in Steel 08Kh18N8D3BR Deformed at a Rate of $1.3 \times 10^{-3} \text{ sec}^{-1}$ to a Strain of 5 and 30% at Various Temperatures

$t_{\text{def}}, ^\circ\text{C}$	Dislocation density, m^{-2}	
	$\varepsilon = 5\%$	$\varepsilon = 30\%$
500	4.0×10^{14}	1.4×10^{15}
620	2.9×10^{14}	1.1×10^{15}
710	3.6×10^{14}	7×10^{14}
Initial state	7×10^{12}	

that at low strain the absolute majority of the generated dislocations is blocked by coherent particles virtually immediately after their formation. The free path of the dislocations seems to be close to the distance between two coherent particles. Accordingly, straining at low degrees of deformation occurs due to continuous generation of new and new dislocations. When the dislocation density in plane accumulations attains a critical value, they start to cut the coherent particles; a PLC effect appears on the $\sigma - \varepsilon$ curves. Collective motion of dislocations increases markedly the free path of a mobile dislocation. As a result, the rate of growth of the dislocation density decreases abruptly (Table 2) and so does the strain hardening factor (Table 1).

As we have mentioned above, the PLC effect manifests itself in the steel studied as discontinuous yielding of types *A* and *E* in the entire range of deformation temperatures and rates used. As a rule, a serrated pattern of types *A* and *E* is a consequence of plane slip having the form of strain bands propagating to great distances [9, 17] and is connected with the interaction between mobile dislocations and interstitial atoms like nitrogen and carbon. According to [18], this type of strain increases considerably the strength of steels of the austenitic class, which can be observed in Fig. 6.

In order to determine the causes of high strength of steel 08Kh18N8D3BR we evaluated the effect of the temperature and rate of deformation on the critical degree of strain and thus on the nature of the serrated patterns of yielding in steel 08Kh18N8D3BR. It is known that ε_{cr} is related to the temperature and rate of deformation through the following expression [19]:

$$\varepsilon_{\text{cr}}^{(m+\beta)} = K \dot{\varepsilon} \exp\left(\frac{Q}{kT}\right), \quad (2)$$

where m and β are the exponents in the dependences $C_v \propto \varepsilon^m$ and $\rho_m \propto \varepsilon^\beta$ (here C_v is the concentration of vacancies, ρ_m is the dislocation density, and ε is the degree of strain), K is a constant, Q is the activation energy, and k is Boltzmann's constant.

Exponent $m + \beta$ in Eq. (2) calculated as the slope of the "positive" part of the double logarithmic dependence $\varepsilon_{\text{cr}} - \dot{\varepsilon}$ (Fig. 8*a*) turned out to be equal to 0.9; this value is typical

TABLE 3. Specific Volume of the Copper Phase and Chemical Composition of the Copper Phase and of the Iron-Enriched Austenite

$t, ^\circ\text{C}$	$V_{\gamma\text{-Cu}}, \%$	Content of elements in $\gamma\text{-Fe}$, wt.%				Content of elements in $\gamma\text{-Cu}$, wt.%			
		Fe	Ni	Cr	Cu	Fe	Ni	Cr	Cu
500	2.8	60	26	10	2.0	0.06	1.7	0.001	98
620	2.3	71	10	15	1.3	0.20	1.4	0.007	98
740	1.5	72	8	17	1.8	0.50	1.3	0.030	98

Note. The data on the specific volume of the copper phase $V_{\gamma\text{-Cu}}$ and of the phase composition of steel 08Kh18N8D3BR have been computed using ThermoCalc.

for interstitial solutions [9]. Using the obtained value of $m + \beta$ and the slope of the curve $\ln(\varepsilon_{\text{cr}}) - 1/T$ (Fig. 8b) we could calculate the activation energy of discontinuous yielding, which turned out to be 94.5 kJ/mole. In some works [17, 20] the activation energy of the PLC effect in austenitic steels is evaluated as 134 – 142 kJ/mole for carbon and/or nitrogen atoms, 84 – 92 kJ/mole for vacancies, 280 kJ/mole for chromium atoms, and 138 kJ/mole for the ‘carbon or/and nitrogen – vacancy’ pair. Comparison of the value of the activation energy of the PLC effect obtained in the present work with the values mentioned shows that in steel 08Kh18N8D3BR the PLC effect is caused either by the motion of vacancies or by the motion of ‘vacancy – interstitial atom pairs.’ Note that in [9, 17, 20] the discontinuous yielding in austenitic steels at 450 – 650°C was controlled by the diffusion of chromium and the strength of these steels was lower than in our work.

Though the causes of the substantial growth in the strength of steel 08Kh18N8D3BR are not completely clear, we may state that in the whole range of temperatures studied copper ensures solid-solution hardening of the steel. Computations with the use of ThermoCalc (Table 3) showed that at a temperature below 750°C the austenite stratifies into solid solutions enriched with iron and copper. The specific volume of the copper phase decreases upon growth in the temperature (Table 3). Joint alloying with copper, niobium, and nitrogen widens the range of cold deformation of the steel toward higher temperatures. This not only promotes growth in the rupture strength of the steel by 90 – 100 MPa, which amounts to 100% of σ_r of steel 304L, but also preserves the conventional yield strength at a level of about 187 MPa to up to 740°C.

CONCLUSIONS

1. The temperature and rate range of occurrence of the Portevin – Le Chatelier effect in steel 08Kh18N8D3BR has been determined as 530 – 650°C at a deformation rate of $1.3 \times 10^{-3} \text{ sec}^{-1}$. The steel manifests the following features of the PLC effect: (a) discontinuous yielding reflected by a serrated form of the stress-strain curve, (b) negative values of the rate sensitivity factor, (c) “normal” dependence of the

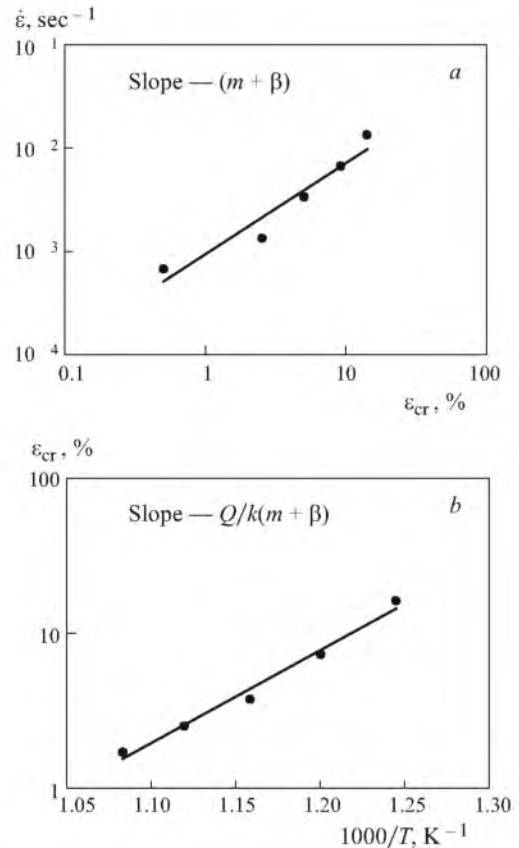


Fig. 8. Dependences of the deformation rate of steel 08Kh18N8D3BR on the critical degree of strain (a) and of the critical degree of strain on the reciprocal temperature (b).

critical degree of strain on the temperature and “normal” and “inverse” dependences on the rate of deformation, and (d) presence of a plateau on the temperature dependence of the yield strength.

2. The discontinuous yielding of the metal is connected with plane slip and formation of strain bands at any temperature and rate of deformation studied.

3. Joint alloying of a steel bearing 18% Cr and 8% Ni with copper, niobium and nitrogen widens the range of cold deformation of the steel toward high temperatures; the yield

strength at 500 – 650°C becomes twice higher than in steel 304L.

4. The dislocation density in the range of occurrence of the Portevin – Le Chatelier effect increases from 7×10^{12} to about $3 \times 10^{14} \text{ m}^{-2}$ in the process of plastic deformation to $\varepsilon = 5\%$. Further plastic deformation until failure increases the dislocation density to about $1.1 \times 10^{15} \text{ m}^{-2}$.

This work has been performed with the use of equipment of the Collective Use Center of the Belgorod State University and with financial support of the Federal Agency for Science and Innovations, Grant No. 02.523.12.3019. The authors are grateful to the worker of the Collective Use Center I. D. Tarasova for performance of the thermal analysis and to the Head of the Department of Physical Metallurgy of Nonferrous Metals of the Moscow Institute for Steel and Alloys A. N. Solonin for the possibility to work with the ThermoCalc software.

REFERENCES

1. K. Laha, J. Kyono, and N. Shinya, "An advanced creep cavitation resistance of Cu-containing 18Cr – 12Ni – Nb austenitic stainless steel," *Scr. Mater.*, **56**, 915 – 918 (2007).
2. Landolt-Bornstein, "Creep properties of heat resistant steels and superalloys Group VIII," *Adv. Mater. Technol.*, **2B**, 260 – 264 (1990).
3. T. Iwasaki, I. Kajigaya, and H. Nakagawa, "Construction planning of 600/620 deg. C USC boiler in Japan," in: *Proc. 4th Int. Conf. Adv. Mater. Technol.*, Fossil Power Plants (2005), pp. 68 – 79.
4. S. Caminada, L. Cipolla, G. Cumino, et al., "Ferritic and austenitic grades for the new generation of steam boiler plants," in: *Proc. 5th Int. Conf. Adv. Mater. Technol.*, Fossil Power Plants (2007), CD-disk.
5. S. Caminada, G. Cumino, L. Cipolla, et al., "Creep properties and microstructural evolution of austenitic TEMPALLOY steels," in: *Creep & Fracture in High Temperature Components, 2nd ECCC Creep Conf.*, DEStech. Publications (2009) , pp. 539 – 550.
6. A. Iseda, H. Okada, H. Semba, and M. Igarashi, "Long-term creep properties and microstructure of Super304H, TP347HFG and HR3C for advanced USC boilers," in: *Proc. 5th Int. Conf. Adv. Mater. Technol.*, Fossil Power Plants (2005), DC-disk.
7. *ASME Boiler and Pressure Vessel Code* (2004), p. 260.
8. O. Sitdikov and R. Kaibyshev, "Dislocation glide and dynamic recrystallization in LiF single crystals," *Mater. Sci. Eng.*, **328**, 147 – 155 (2002).
9. P. Rodriguez, "Serrated plastic flow," *Bull. Mater. Sci.*, **6**(4), 653 – 663 (1984).
10. Y. Brechet and Y. Estrin, "On a pseudo Portevin – Le Chatelier effect," *Scr. Metall. Mater.*, **31**, 185 – 190 (1994).
11. Y. Brechet and Y. Estrin, "Pseudo Portevin – Le Chatelier effect in ordered alloys," *Scr. Mater.*, **35**, 217 – 223 (1996).
12. *MIL-HDBK-5J, Metallic Materials and Elements for Aerospace Vehicle Structures* (2003), pp. 2 – 225.
13. F. Abe, "18Cr – 8Ni steel. Austenitic stainless steels: creep and rupture data of heat resistant steels," in: *Creep Properties of Heat Resistant Steels and Superalloys*, Springer, Berlin (2004), pp. 206 – 226.
14. M. Igarashi, "Fine-grained 18Cr – 12Ni – Nb steel. Austenitic stainless steels: creep and rupture data of heat resistant steels," in: *Creep Properties of Heat Resistant Steels and Superalloys*, Springer, Berlin (2004), pp. 251 – 257.
15. B. Bay, N. Hansen, D. A. Hughes, and D. Kuhlmann-Wilsdorf, "Evolution of f.c.c. deformation structures in polyslip," *Acta Metall. Mater.*, **40**, 205 – 219 (1992).
16. O. A. Kaibyshev and R. Z. Valiev, *Grain Boundaries and Properties of Metals* [in Russian], Metallurgiya, Moscow (1987).
17. S. G. Hong and S. B. Lee, "The tensile and low-cycle fatigue behavior of cold worked 316L stainless steel: influence of dynamic strain aging," *Int. J. Fatigue*, **26**, 899 – 910 (2004).
18. J. W. Simmomm, "Overview: high-nitrogen alloying of stainless steel," *Mater. Sci. Eng.*, **A207**, 159 – 169 (1996).
19. A. Van den Beukel, "On the mechanism of serrated yielding and dynamic strain aging," *Acta Metall.*, **28**, 965 – 969 (1980).
20. S. G. Hong and S. B. Lee, "Mechanism of dynamic strain aging and characterization of its effect on the low-cycle fatigue behavior in type 316L stainless steel," *J. Nucl. Mater.*, **340**, 307 – 314 (2005).